RESEARCH ON BUILDING A GENERAL MODEL OF ACTIVE ANTI-ROLL SYSTEM IN TRUCKS

Vu Van Dinh[1], Nguyen Trung Nguyen[2], Pham Tat Thang[2], Vu Van Tan[2,*]

DOI: https://doi.org/10.57001/huih5804.2026.013

ABSTRACT

The active anti-roll system plays an important role in enhancing vehicle safety. This paper presents a study and the development of a generalized model of a two axle truck equipped with an active anti-roll system. Initially, a model of a hydraulic actuator with electronic servo valve control is developed, in which the control input is the electric current. Subsequently, a full vehicle model of the two axle truck, employing four actuators with two actuators mounted on each axle, is constructed (two actuators for the front axles and two actuators for the rear axles), with the input disturbance is the steering angle. Simulation results and analyses in both the time and frequency domains in different velocities clearly demonstrate the dynamic characteristics of the actuators. This study provides a foundation for the future design and implementation of control strategies for the active roll stability system.

Keywords: *Active anti-roll system, truck, electro-hydraulic actuator, active anti-roll bar system.*

[1]Division of Mechanical Engineering, University of Transport and Communications - Campus in Ho Chi Minh City, Viet Nam

[2]Faculty of Mechanical Engineering, University of Transport and Communications, Viet Nam

[*]Email: vvtan@utc.edu.vn

Received: 15/7/2025

Revised: 25/11/2025

Accepted: 28/01/2026

1. INTRODUCTION

Rollover accidents of heavy vehicles are a critical issue in global road safety, often resulting in severe consequences in terms of human casualties and property damage. According to a report by the National Highway Traffic Safety Administration (NHTSA), in 2022, there were over 5,936 fatalities and approximately 160,608 injuries associated with heavy-duty trucks, primarily attributed to rollover phenomena. This figure represents an increase of about 3% compared to 2021. Similarly, in the European Union, the year 2023 saw over 2,899 fatalities from accidents involving trucks, constituting nearly 14% of all traffic-related deaths, despite heavy vehicles accounting for only a small proportion of the total fleet in circulation [1]. During 2024, Vietnam recorded 21,532 road traffic accidents nationwide, leading to 9,954 fatalities and 16,044 injuries, based on data from the Traffic Police Department - Ministry of Public Security (compiled by the National Traffic Safety Committee) [2].

The primary causes of rollover phenomenon include heavy trucks cornering at high speeds, abrupt lane changes, or sudden steering maneuvers, along with load-related factors such as a high cargo center of gravity or uneven weight distribution [3]. Due to the inherent design characteristics of heavy vehicles (high center of gravity, narrow track width), many rollover scenarios cannot be mitigated solely through driver skill or warning systems [4]. This highlights the need for active safety systems capable of timely intervention.

Although modern safety systems for suspension, braking, and steering have undergone significant advancements, they still exhibit limitations in rollover prevention. Specifically, passive anti-roll bars offer only a fixed stiffness, creating a fundamental trade-off between the requirement for enhanced roll stability and the assurance of ride comfort [5]. Increasing stiffness improves rollover resistance but compromises ride quality, whereas softening the suspension to improve comfort elevates the risk of rollover. Meanwhile, modern electronic systems such as ABS and ESC primarily provide indirect intervention by reducing vehicle speed or modulating engine torque upon detecting a potential loss of stability, rather than generating a direct anti-roll moment. This limits their effectiveness in emergency situations, such as sharp cornering maneuvers with a heavily loaded vehicle.

To solve these problems, the active anti-roll system has become an important solution for greatly improving the stability of heavy trucks. This system uses hydraulic or electric actuators, controlled by a computer, to create an active anti-roll force. This makes the vehicle much harder to roll over compared to traditional, non-active systems.

Previous research around the world has shown this solution works well. For example, a research team led by Professor David Cebon at the University of Cambridge built a test truck with an active stability system to improve its resistance to rolling over [5]. Their tests showed the active system not only reduced the risk of rollover but also reduced the dynamic loads exerted on the road surface. Additionally, modern control methods like optimal control, robust H_∞ control, and LPV control have been used to make these active systems perform even better [9]. The PhD research by Vu Van Tan proposed an H_∞/LPV controller for the active anti-roll bar, enabling the vehicle to better adapt to rollover risks in different real-world driving conditions [6].

These research results confirm that active anti-roll systems are becoming more and more important for making heavy trucks safer. Because of this, this paper focuses on creating a general model for an active anti-roll system on a heavy truck. This model will be a starting point for creating new control methods that can effectively prevent rollovers.

2. ELECTRONIC SERVO-VALVE HYDRAULIC ACTUATOR MODELING

In the active anti-roll system for heavy vehicles, the actuator plays an important role in generating active anti-roll moments. This actuator is typically an Electronic Servo-Valve Hydraulic (ESVH) system, which consists of an electronic servo-valve and hydraulic cylinders mounted between the sprung and unsprung masses at each axle. It is tasked with generating an actuator force by creating a difference of pressure between the two chambers of the cylinder.

Figure 1 illustrates the diagram of a typical ESVH actuator used in an active anti-roll system. The electronic servo-valve is controlled by an electrical current i, which generates a spool valve displacement, X_v. As the spool valve moves, it distributes high pressure oil into the two chambers of the hydraulic cylinder. This creates a difference of pressure ΔP, which produces the actuator force F_{act} given by the following equation:

$$F_{act} = A_P \Delta P \tag{1}$$

Where: F_{act} is the actuator force; A_p is the area of the piston, and ΔP is the difference of pressure between the two chambers of the hydraulic cylinder.

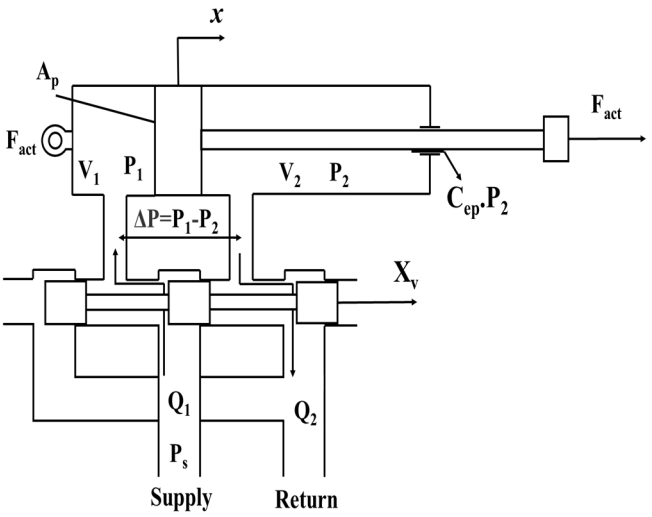

Figure 1. Diagram of the ESVH actuator

To accurately describe the dynamics of the Electronic Servo-Valve Hydraulic (ESVH) actuator, the model can be summarized by the following system of differential equations:

$$\begin{cases} F_{act} = A_P \Delta P \\ \dfrac{V_t}{4\beta_e}\dfrac{d\Delta P}{dt} + \left(K_P + C_{tp}\right)\Delta P - K_x X_v + A_P \dfrac{dx}{dt} = 0 \\ \dfrac{dX_v}{dt} + \dfrac{1}{\tau}X_v - \dfrac{K_v}{\tau} i = 0 \end{cases} \tag{2}$$

Where: V_t is the total volume of trapped oil in the actuator; β_e is the effective bulk modulus of the oil; K_p, K_x are the total flow pressure coefficient and the valve flow gain, respectively; C_{tp} is the total leakage coefficient of the hydraulic cylinder; A_p is the area of the piston; τ, K_v are the time constant and gain of the servo-valve model, respectively; i is the input current.

Therefore, the actuator model described above provides a solid theoretical basis for designing control strategies for the active anti-roll force. This ensures the active anti-roll system on heavy trucks can adapt quickly and accurately under real driving conditions.

3. HEAVY TRUCK MODEL USING ACTIVE ANTI-ROLL SYSTEM

3.1. Heavy Truck Model

To investigate the effectiveness of the active anti-roll system, this paper uses a dynamic model of a two-axle heavy truck, as illustrated in Figure 2. This model allows

for the accurate simulation of the vehicle's lateral roll oscillations when subjected to maneuvers that could potentially cause a rollover.

Figure 2 describes the two-axle truck model used for studying roll stability. It consists of three basic parts: m_s is the sprung mass, m_{uf} is the unsprung mass at the front axle, and m_{ur} is the unsprung mass at the rear axle. Overall, the model has five degrees of freedom. The sprung mass can rotate about the roll axis (O_x). The location of this roll axis depends on the kinematic properties of the front and rear suspension systems. The unsprung masses can also roll, an effect which is heavily dependent on the tire stiffness. The leaf springs, dampers, and passive anti-roll bars generate moments between the sprung and unsprung masses in response to roll motions. The active anti-roll system generates additional (controlled) moments between the sprung and unsprung masses to enhance the vehicle's roll stability.

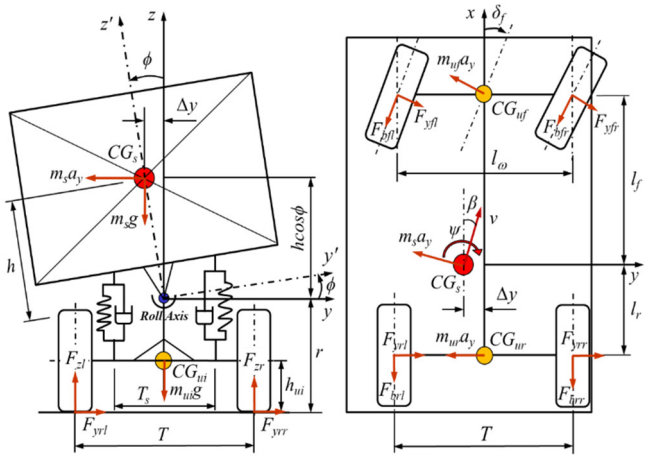

Figure 2. The two-axle heavy truck model [16]

The differential equations of motion for the vehicle model are formalized as follows:

$$\begin{cases} m.v.\left(\dot{\beta}+\dot{\psi}\right)-m_s.h.\ddot{\varphi}=F_{yf}+F_{yr} \\ -I_{xz}.\ddot{\varphi}+I_{zz}.\ddot{\psi}=F_{yf}.l_f-F_{yr}.l_r \\ \left(I_{xx}+m_s.h^2\right).\ddot{\varphi}-I_{xz}.\ddot{\psi}=m_s.g.h.\varphi+m_s.v.h.\left(\dot{\beta}+\dot{\psi}\right)-k_f.\left(\varphi-\varphi_{uf}\right) \\ -c_f.\left(\dot{\varphi}-\dot{\varphi}_{uf}\right)+M_{ARf}+M_f-k_r.\left(\varphi-\varphi_{ur}\right)-c_r.\left(\dot{\varphi}-\dot{\varphi}_{ur}\right) \\ +M_{ARr}+M_r-r.F_{yf}=m_{uf}.v.\left(r-h_{uf}\right).\left(\dot{\beta}+\dot{\psi}\right)+m_{uf}.g.h_{uf}.\varphi_{uf} \\ -k_{uf}.\varphi_{uf}+k_f.\left(\varphi-\varphi_{uf}\right)+c_f.\left(\dot{\varphi}-\dot{\varphi}_{uf}\right)+M_{ARf}+M_f \\ -r.F_{yr}=m_{ur}.v.\left(r-h_{ur}\right).\left(\dot{\beta}+\dot{\psi}\right)-m_{ur}.g.h_{ur}.\varphi_{ur} \\ -k_{ur}.\varphi_{ur}+k_r.\left(\varphi-\varphi_{ur}\right)+c_r.\left(\dot{\varphi}-\dot{\varphi}_{ur}\right)+M_{ARr}+M_r \end{cases} \quad (3)$$

where M_{ARf} and M_{ARr} are the moments from the passive anti-roll bars at the two axles, while M_f and M_r are the moments generated by the active anti-roll system.

3.2. Building an integrated model of heavy truck and actuators

Figure 3 presents the overall model of the two-axle heavy truck integrated with the active anti-roll system. This model includes the vehicle body with its general equations of motion (Equation 3), combined with four Electronic Servo-Valve Hydraulic (ESVH) actuators (two at the front axle and two at the rear axle). Each actuator is described by its own dynamic equations (Equation 2).

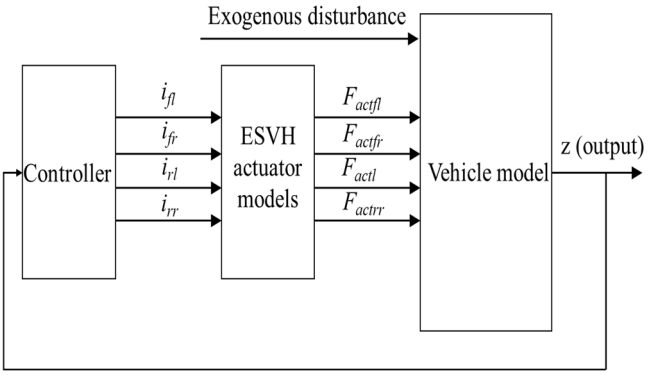

Figure 3. Diagram of the fully integrated model with the active anti-roll system

In the control structure, a central controller receives feedback signals from the system (output vector z). It then calculates and generates the input current signals for the servo-valves: i_{fl}, i_{fr} at the front axle and i_{rl}, i_{rr} at the rear axle. These control signals act on the servo-valves, changing the pressure difference in the hydraulic cylinders, which in turn generates the corresponding actuator forces F_{actfl}, F_{actfr}, F_{actrl}, F_{actrr}.

These actuator forces create the active anti-roll moments around the vehicle's roll axis. The active torque at the front axle is determined by the following expression:

$$\begin{aligned} M_f &= -l_{act}F_{actfl}+l_{act}F_{actfr} \\ &= -l_{act}A_p\Delta_{Pfl}+l_{act}A_p\Delta_{Pfr} \end{aligned} \quad (4)$$

And similarly, the torque at the rear axle is:

$$\begin{aligned} M_r &= -l_{act}F_{actrl}+l_{act}F_{actrr} \\ &= -l_{act}A_p\Delta_{Prl}+l_{act}A_p\Delta_{Prr} \end{aligned} \quad (5)$$

Where, l_{act} is half the distance between the two actuators at each axle. The terms ΔP_{fl} and ΔP_{fr} are the pressure differences in the left and right hydraulic cylinders of the front axle, respectively; similarly, ΔP_{rl} and ΔP_{rr} are the pressure differences in the left and right cylinders of the rear axle.

The general dynamical equations of the active anti-roll system in the fully integrated model are presented in equation (6). From the equations above, the full dynamical equations of the ESVH actuators are shown as:

$$\begin{cases} \frac{V_t}{4\beta_e}\dot{\Delta}_{Pfl}+(K_P+C_{tp})\Delta_{Pfl}-K_xX_{vfl}-A_pl_{act}\dot{\phi}+A_pl_{act}\dot{\phi}_{uf}=0 \\ \dot{X}_{vfl}+\frac{1}{\tau}X_{vfl}-\frac{K_v}{\tau}i_{fl}=0 \\ \frac{V_t}{4\beta_e}\dot{\Delta}_{Pfr}+(K_P+C_{tp})\Delta_{Pfr}-K_xX_{vfr}-A_pl_{act}\dot{\phi}+A_pl_{act}\dot{\phi}_{uf}=0 \\ \dot{X}_{vfr}+\frac{1}{\tau}X_{vfr}-\frac{K_v}{\tau}i_{fr}=0 \\ \frac{V_t}{4\beta_e}\dot{\Delta}_{Prl}+(K_P+C_{tp})\Delta_{Prl}-K_xX_{vrl}-A_pl_{act}\dot{\phi}+A_pl_{act}\dot{\phi}_{ur}=0 \\ \dot{X}_{vrl}+\frac{1}{\tau}X_{vrl}-\frac{K_v}{\tau}i_{rl}=0 \\ \frac{V_t}{4\beta_e}\dot{\Delta}_{Prr}+(K_P+C_{tp})\Delta_{Prr}-K_xX_{vrr}-A_pl_{act}\dot{\phi}+A_pl_{act}\dot{\phi}_{ur}=0 \\ \dot{X}_{vrr}+\frac{1}{\tau}X_{vrr}-\frac{K_v}{\tau}i_{rr}=0 \end{cases} \quad (6)$$

The combination of equations (3) and (6) forms the system of differential equations that fully describes the dynamics of the integrated vehicle-actuator model. This system is then written in the Linear Time-Invariant (LTI) state-space representation form as:

$$\dot{x}=Ax+B_1\mathrm{w}+B_2u \quad (7)$$

where the state vector is given by:

$$x=\left[\beta\ \ \dot{\psi}\ \ \phi\ \ \dot{\phi}\ \ \phi_{uf}\ \ \phi_{ur}\ \ \Delta_{Pfl}\ \ X_{vfl}\ \ \Delta_{Pfr}\ \ X_{vfr}\ \ \Delta_{Prl}\ \ X_{vrl}\ \ \Delta_{Prr}\ \ X_{vrr}\right]^T$$

The exogenous disturbance (steering angle) is: $\mathrm{w}=[\delta_f]$; and the control inputs (input currents) are: $i=\left[i_{fl}\ \ i_{fr}\ \ i_{rl}\ \ i_{rr}\right]^T$; The matrices in equation (7) are defined as: $A=E^{-1}A_0$, $B_1=E^{-1}B_{01}$ và $B_2=E^{-1}B_{02}$.

To simplify the setup of these matrices, some characteristic notations are defined as follows:

$$Y_{\beta f}=-\mu.C_f,\ Y_{\dot{\psi}f}=-\mu.\frac{l_f.C_f}{v},$$

$$Y_{\beta r}=-\mu.C_r,\ Y_{\dot{\psi}r}=\mu.\frac{l_r.C_r}{v},$$

$$Y_\beta=Y_{\beta f}+Y_{\beta r}=-\mu.(C_f+C_r),$$

$$Y_{\dot{\psi}}=Y_{\dot{\psi}f}+Y_{\dot{\psi}r}=\mu.(\frac{C_r.l_r-C_f.l_f}{v}),$$

$$Y_\delta=\mu.C,\ N_\beta=\mu.(l_r.C_r-l_f.C_f),$$

$$N_{\dot{\psi}}=-\mu.(\frac{l_f^2.C_f+l_r^2.C_r}{v}),\ N_\delta=\mu.l_f.C_f.$$

The matrices B_{01}, B_{02} are composed as follows:

$$B_{01}=\begin{bmatrix} Y_\delta \\ N_\delta \\ 0 \\ rY_\delta \\ 0 \\ 0 \\ 0 \\ 0 \\ 0 \\ 0 \\ 0 \\ 0 \\ 0 \\ 0 \end{bmatrix} \qquad B_{02}=\begin{bmatrix} 0 & 0 & 0 & 0 \\ 0 & 0 & 0 & 0 \\ 0 & 0 & 0 & 0 \\ 0 & 0 & 0 & 0 \\ 0 & 0 & 0 & 0 \\ 0 & 0 & 0 & 0 \\ \frac{Kv}{\tau} & 0 & 0 & 0 \\ 0 & 0 & 0 & 0 \\ 0 & \frac{Kv}{\tau} & 0 & 0 \\ 0 & 0 & 0 & 0 \\ 0 & 0 & \frac{Kv}{\tau} & 0 \\ 0 & 0 & 0 & 0 \\ 0 & 0 & 0 & \frac{Kv}{\tau} \end{bmatrix}$$

The matrix $E=\left[E_1, E_2\right]$, where the sub-matrices are:

$$E_1=\begin{bmatrix} mv & 0 & 0 & -m_sh & 0 \\ 0 & I_{zz} & 0 & -I_{xz} & 0 \\ -m_svh & -I_{xz} & 0 & I_{xx}+m_sh^2 & -b_f \\ -m_{uf}v(r-h_{uf}) & 0 & 0 & 0 & b_f \\ -m_{ur}v(r-h_{ur}) & 0 & 0 & 0 & 0 \\ 0 & 0 & 1 & 0 & 0 \\ 0 & 0 & 0 & 0 & A_Pl_{act} \\ 0 & 0 & 0 & 0 & 0 \\ 0 & 0 & 0 & 0 & -A_Pl_{act} \\ 0 & 0 & 0 & 0 & 0 \\ 0 & 0 & 0 & 0 & 0 \\ 0 & 0 & 0 & 0 & 0 \\ 0 & 0 & 0 & 0 & 0 \\ 0 & 0 & 0 & 0 & 0 \end{bmatrix}$$

$$E_2 = \begin{bmatrix} 0 & 0 & 0 & 0 & 0 & 0 & 0 & 0 & 0 \\ 0 & 0 & 0 & 0 & 0 & 0 & 0 & 0 & 0 \\ -b_r & 0 & 0 & 0 & 0 & 0 & 0 & 0 & 0 \\ 0 & 0 & 0 & 0 & 0 & 0 & 0 & 0 & 0 \\ b_r & 0 & 0 & 0 & 0 & 0 & 0 & 0 & 0 \\ 0 & 0 & 0 & 0 & 0 & 0 & 0 & 0 & 0 \\ 0 & \frac{V_t}{4\beta e} & 0 & 0 & 0 & 0 & 0 & 0 & 0 \\ 0 & 0 & 1 & 0 & 0 & 0 & 0 & 0 & 0 \\ 0 & 0 & 0 & \frac{V_t}{4\beta e} & 0 & 0 & 0 & 0 & 0 \\ 0 & 0 & 0 & 0 & 1 & 0 & 0 & 0 & 0 \\ A_P l_{act} & 0 & 0 & 0 & 0 & \frac{V_t}{4\beta e} & 0 & 0 & 0 \\ 0 & 0 & 0 & 0 & 0 & 0 & 1 & 0 & 0 \\ -A_P l_{act} & 0 & 0 & 0 & 0 & 0 & 0 & \frac{V_t}{4\beta e} & 0 \\ 0 & 0 & 0 & 0 & 0 & 0 & 0 & 0 & 1 \end{bmatrix}$$

The matrix $A_0 = \left[A_{01}, A_{02}, A_{03} \right]$ is defined as follows:

$$A_{01} = \begin{bmatrix} Y_\beta & Y_{\dot{\psi}} - mv & 0 & 0 \\ N_\beta & N_{\dot{\psi}} & 0 & 0 \\ 0 & m_s vh & m_s gh - k_f - k_r & -(b_f + b_r) \\ rY_{\beta f} & m_{uf} v(r - h_{uf}) + rY_{\dot{\psi} f} & k_f & b_f \\ rY_{\beta r} & m_{ur} v(r - h_{ur}) + rY_{\dot{\psi} r} & k_r & b_r \\ 0 & 0 & 0 & 1 \\ 0 & 0 & 0 & l_{act} A_P \\ 0 & 0 & 0 & 0 \\ 0 & 0 & 0 & -l_{act} A_P \\ 0 & 0 & 0 & 0 \\ 0 & 0 & 0 & l_{act} A_P \\ 0 & 0 & 0 & 0 \\ 0 & 0 & 0 & -l_{act} A_P \\ 0 & 0 & 0 & 0 \end{bmatrix}$$

$$A_{02} = \begin{bmatrix} 0 & 0 & 0 & 0 \\ 0 & 0 & 0 & 0 \\ k_f & k_r & -l_{act} A_P & 0 \\ m_{uf} g h_{uf} - k_f - k_{uf} & 0 & -l_{act} A_P & 0 \\ 0 & -(m_{ur} g h_{ur} + k_r + k_{ur}) & 0 & 0 \\ 0 & 0 & 0 & 0 \\ 0 & 0 & -(K_P + C_{tp}) & K_x \\ 0 & 0 & 0 & \frac{1}{\tau} \\ 0 & 0 & 0 & 0 \\ 0 & 0 & 0 & 0 \\ 0 & 0 & 0 & 0 \\ 0 & 0 & 0 & 0 \\ 0 & 0 & 0 & 0 \\ 0 & 0 & 0 & 0 \end{bmatrix}$$

$$A_{03} = \begin{bmatrix} 0 & 0 & 0 & 0 & 0 & 0 \\ 0 & 0 & 0 & 0 & 0 & 0 \\ l_{act} A_P & 0 & -l_{act} A_P & 0 & l_{act} A_P & 0 \\ l_{act} A_P & 0 & 0 & 0 & 0 & 0 \\ 0 & 0 & -l_{act} A_P & 0 & l_{act} A_P & 0 \\ 0 & 0 & 0 & 0 & 0 & 0 \\ 0 & 0 & 0 & 0 & 0 & 0 \\ 0 & 0 & 0 & 0 & 0 & 0 \\ -(K_P + C_{tp}) & K_x & 0 & 0 & 0 & 0 \\ 0 & -\frac{1}{\tau} & 0 & 0 & 0 & 0 \\ 0 & 0 & -(K_P + C_{tp}) & K_x & 0 & 0 \\ 0 & 0 & 0 & -\frac{1}{\tau} & 0 & 0 \\ 0 & 0 & 0 & 0 & -(K_P + C_{tp}) & K_x \\ 0 & 0 & 0 & 0 & 0 & -\frac{1}{\tau} \end{bmatrix}$$

In an active anti-roll system, the two actuators of an axle must generate forces of equal magnitude but in opposite directions. This is a mandatory requirement to avoid generating a net vertical force on the sprung and unsprung masses, which would cause unwanted vertical acceleration. If this condition is not met, the system could cause unwanted vibrations, affecting the vehicle's ride comfort and stability. Therefore, the proposed fully integrated model must be verified in the frequency domain to ensure the accuracy and effectiveness of this principle.

4. SIMULATION RESULTS AND EVALUATION

4.1. Simulation results in the frequency domain

To verify the fully integrated model and evaluate the dynamic characteristics of the active anti-roll system, an analysis in the frequency domain is performed. The simulations are conducted at three different vehicle speeds: 20km/h, 40km/h, and 60km/h, in order to investigate the influence of velocity on the system's response.

Figures 4 and 5 show the frequency responses of the left and right Electronic Servo-Valve Hydraulic (ESVH) actuators at the front and rear axles. These plots illustrate the relationship between the steering angle input (δ_f) and the actuator's output variables, including the actuator force applied to the vehicle model (F_{act}), the load flow through the hydraulic cylinder (Q_L), the spool valve displacement (X_v), và and the input current (i).

(a) $F_{act,f}$

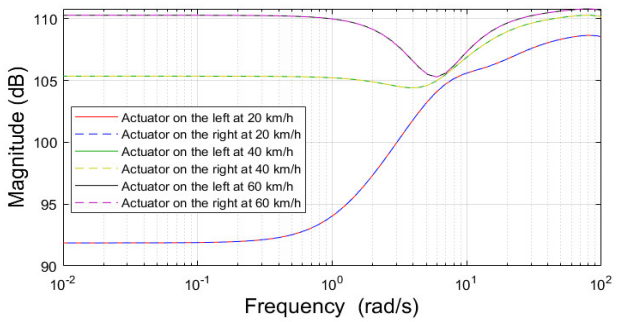

(b) $Q_{L,f}$

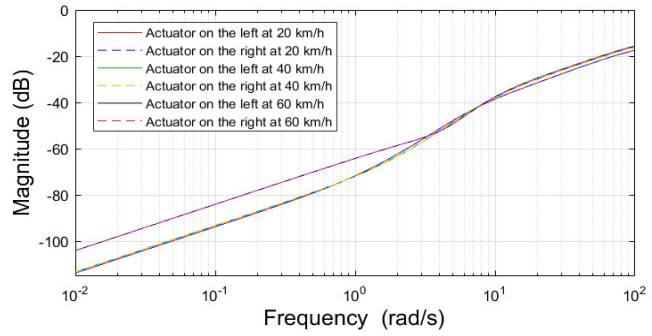

(c) $X_{v,f}$

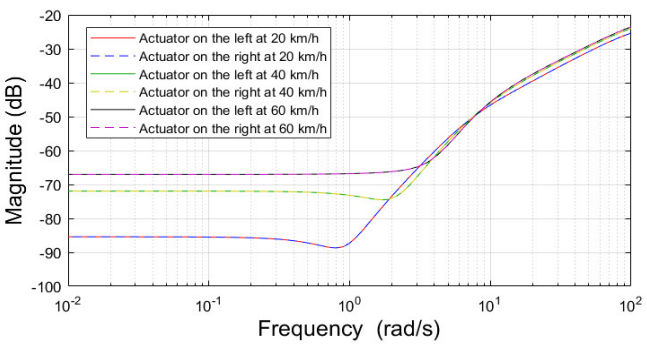

(d) i_f

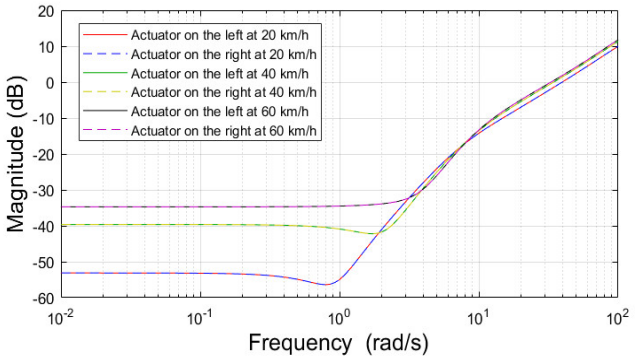

Figure 4. Frequency responses of the ESVH actuators at the front axle at different speeds

(a) $F_{act,r}$

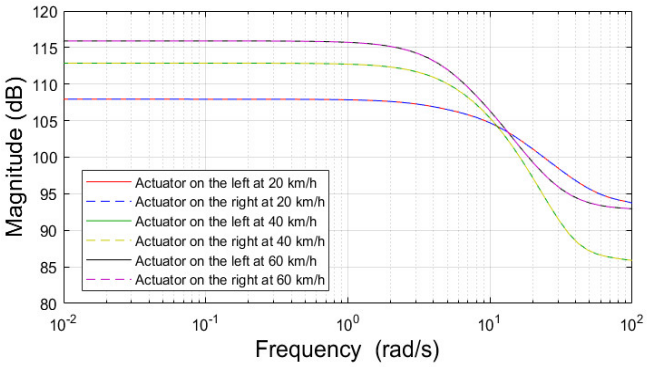

(b) $Q_{L,r}$

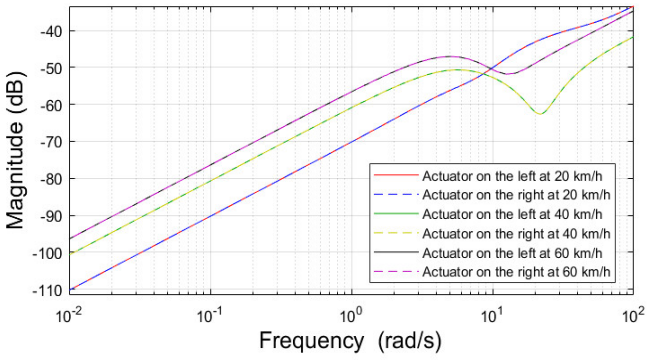

(c) $X_{v,r}$

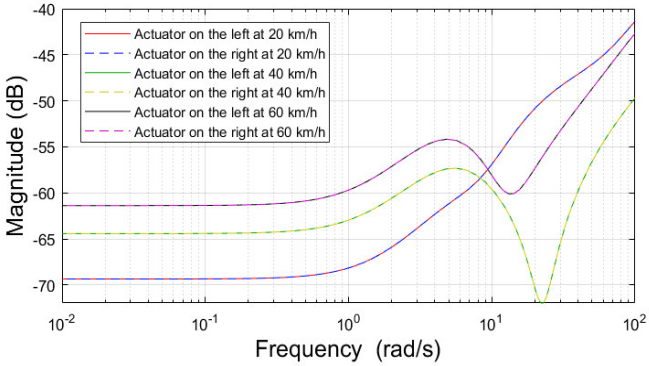

(d) i_r

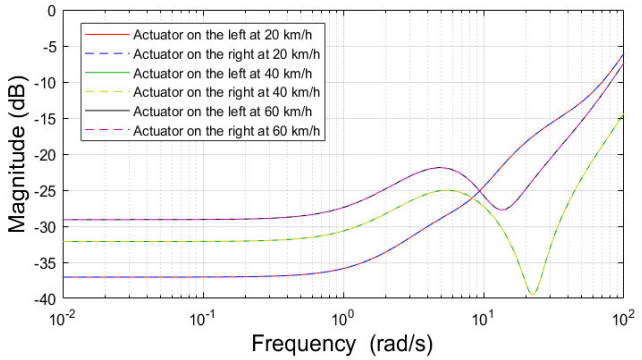

Figure 5. Frequency responses of the ESVH actuators at the rear axle at different speeds

The frequency response analysis in Figures 4 and 5 shows identical amplitude characteristics between the left and right actuators at each axle. This symmetrical characteristic implies that the actuator forces have the same magnitude, thereby forming a force couple that generates an effective anti-roll moment. The cancellation of the net vertical force ensures the system does not influence vertical oscillations, which resolves the conflict between improving roll stability and maintaining ride comfort. Furthermore, the increase in the magnitude of the F_{act} force is proportional to the vehicle's velocity, which is consistent with basic dynamic principles. These results provide strong evidence that validates the correctness of the developed mathematical model.

4.2. Simulation results in the time domain

In this section, the authors evaluate the actuator characteristics as the vehicle performs a double lane change maneuver to avoid an obstacle at a speed of 60km/h. The vehicle's trajectory is shown in Figure 6.

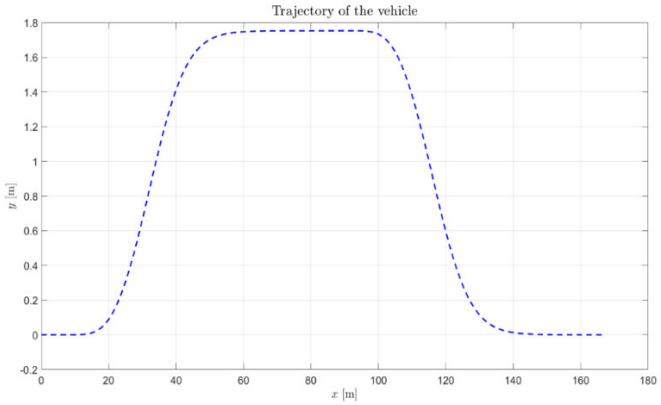

Figure 6. Trajectory of the vehicle

The characteristics of the actuators at the two axles are shown for the front axle in Figure 7 and for the rear axle in Figure 8.

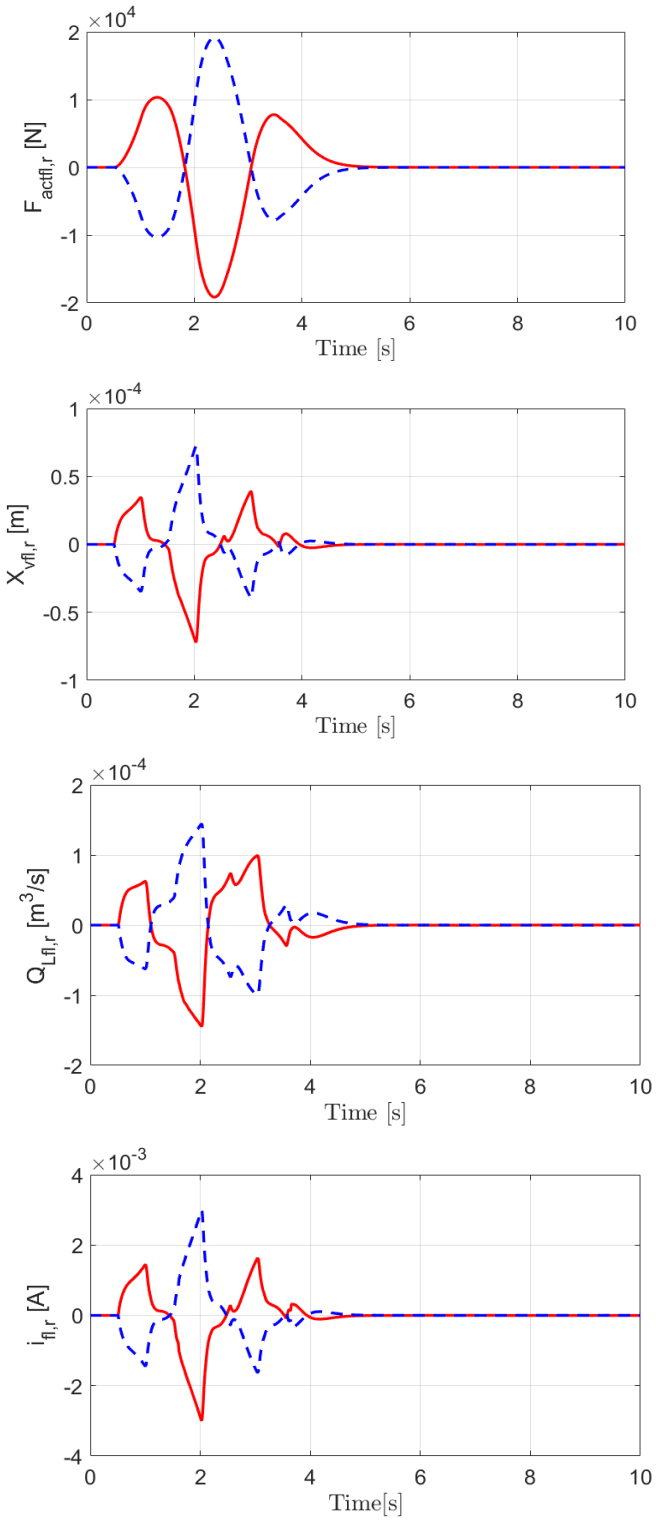

Figure 7. Time response of the front axle actuators

An analysis of Figures 7 and 8 shows a perfect symmetry in the signals from the two actuators on the same axle: the response of the right actuator is the inverse of the left one. This relationship, mathematically represented as $F_{act,l(t)} = -F_{act,r(t)}$ and similarly for other state variables, is maintained throughout the maneuver.

This proves that the actuator forces are always equal in magnitude and opposite in direction, confirming the system's symmetry under dynamic conditions. The time domain simulation results clearly correspond with the frequency-domain results shown in Figures 4 and 5.

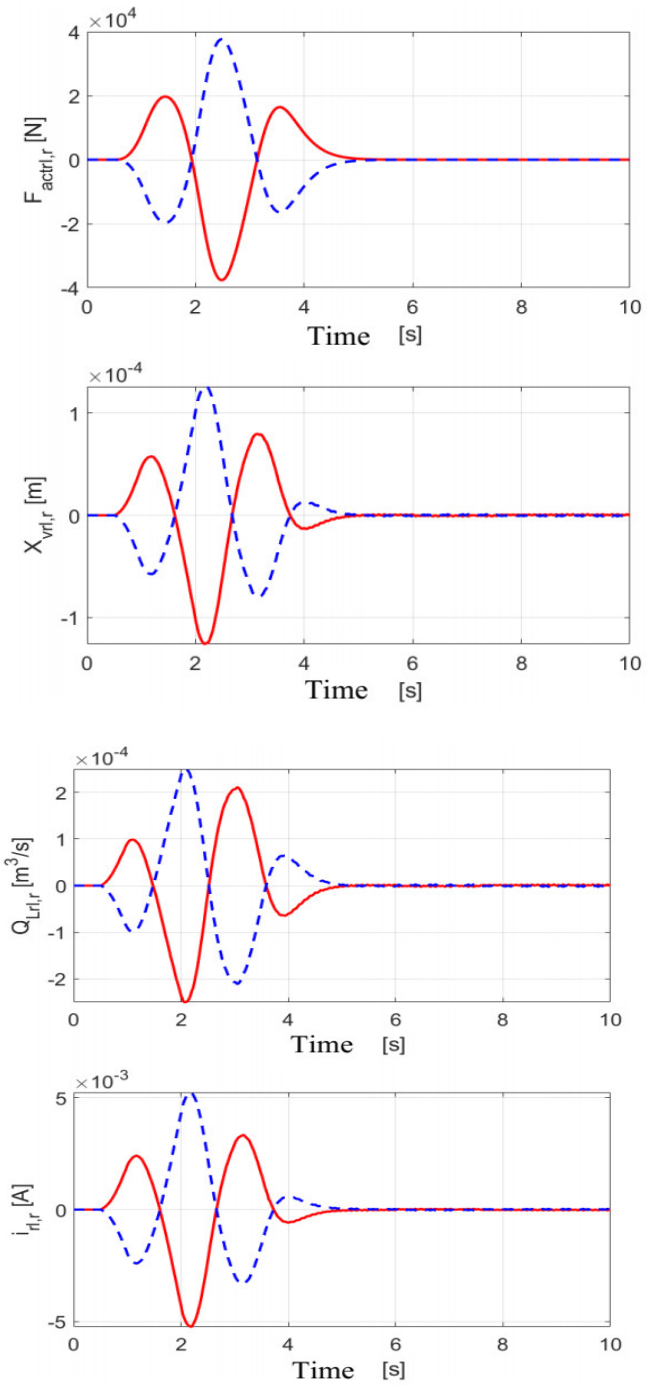

Figure 8. Time response of the rear axle actuators

5. CONCLUSIONS

This paper has presented the development of a fully integrated model of a two-axle heavy truck using an active anti-roll system. In this model, the system employs four electro-hydraulic actuators, each consisting of a hydraulic cylinder controlled by a servo-valve, with two such actuators used in parallel on each axle. The model was then verified and evaluated in both the frequency and time domains at different velocities. The simulation results have clearly shown the characteristics of the actuator and the requirements needed for its application to a real vehicle model.

The next research direction is to develop and compare different control strategies to evaluate the effectiveness of the active anti-roll system under different driving scenarios.

ACKNOWLEDGEMENT

The research is supported by the Ministry of Education and Training (B2025-GHA-09).

REFERENCES

[1]. National Center for Statistics and Analysis, *Large Trucks: 2022 Data*. National Highway Traffic Safety Administration, Washington, DC, USA, Rep. DOT HS 813 588, Jul. 2024. [Online]. Available: https://crashstats.nhtsa.dot.gov/Api/Public/Publication/813588

[2]. National Traffic Safety Committee, "Nearly 10,000 people died from traffic accidents in 2024" (in Vietnamese), *The People's Representative Newspaper*, 2024. [Online]. Available: https://daibieunhandan.vn/gan-10-000-nguoi-chet-vi-tai-nan-giao-thong-trong-nam-2024-i323603.html

[3]. A. J. McKnight, G. T. Bahouth, "Analysis of large truck rollover crashes," *Annals of Advances in Automotive Medicine*, 52, 281-296, 2008.

[4]. D. Cebon, C. Winkler, "Multiple-sensor systems for heavy vehicle stability," *Vehicle System Dynamics*, 23, 5, 341-368, 1994.

[5]. A. J. P. Miège, D. Cebon, "Active roll control of an experimental articulated vehicle," in *Proc. IMechE Part D: Journal of Automobile Engineering*, 219, 6, 791-806, 2005.

[6]. V. T. Vu, *Enhancing the roll stability of heavy vehicles by using an active anti-roll bar system*. Ph.D. dissertation, GIPSA-Lab, Univ. Grenoble Alpes, Grenoble, France, 2017.

[7]. V. T. Vu, O. Sename, L. Dugard, P. Gaspar, "H_∞/LPV controller design for an active anti-roll bar system of heavy vehicles using parameter dependent weighting functions," *Heliyon*, 5, 6, Art. no. e01827, 2019.

[8]. B. Varga, B. Németh, P. Gáspár, "Control design of anti-roll bar actuator based on constrained LQ method," in *Proc. IEEE 14th Int. Symp. Comput. Intell. Informatics (CINTI)*, Budapest, Hungary, pp. 217-222, 2013.

[9]. V. T. Vu, O. Sename, L. Dugard, P. Gaspar, "An Investigation into the Oil Leakage Effect Inside the Electronic Servovalve for an H_∞/LPV Active Anti-roll Bar System," *International Journal of Control, Automation and Systems*, 17, 2917-2928, 2019.

[10]. H. Agrawal, J. Gustafsson, *Investigation of Active Anti-Roll Bars and Development of Control Algorithm.* M.S. thesis, Vehicle Eng., KTH Royal Inst. Technol., Stockholm, Sweden, 2017.

[11]. E. J. Stone, D. Cebon, "An Experimental Semi-Active Anti-roll System," in *Proc. IMechE, Part D: Journal of Automobile Engineering*, 222, no. D12, 2415-2433, 2008.

[12]. B. P. Jeppesen, D. Cebon, "Application of Observer-Based Fault Detection in Vehicle Roll Control," *Vehicle System Dynamics*, 47, 4, 465-495, 2009.

[13]. E. J. Stone, D. Cebon, "Control of Semi-Active Anti-roll Systems on Heavy Vehicles," *Vehicle System Dynamics*, 48, 10, 1215-1243, 2010.

[14]. H. H. Huang, K. Y. Rama, A. G. Dennis, "Active roll control for rollover prevention of heavy articulated vehicles with multiple-rollover-index minimisation," *Vehicle System Dynamics*, 50, 3, 471-493, 2011.

[15]. D. Sampson, D. Cebon, "Active Roll Control of Single Unit Heavy Road Vehicles," *Vehicle System Dynamics*, 40, 229-270, 2003.

[16]. V. V. Tan, P. T. Thang, D. T. Tu, K. D. Thinh, "Combining Optimal Controller and Luenberger Observer for an Active Roll Control System on Trucks to Avoid Rollover at High Speeds," *Shock and Vibration*, 2024, Art. ID 4153900, 2024.

[17]. A. J. P. Miège, *Development of Active Anti-Roll Control for Heavy Vehicles*. Ph.D. dissertation, Dept. Eng., Univ. of Cambridge, Cambridge, U.K., 2000.

[18]. N. Ikhsan, A. Saifizul, R. Ramli, "The effect of vehicle and road conditions on rollover of commercial heavy vehicles during cornering: A simulation approach," *Sustainability*, 13, 11, Art. no. 6337, 2021.